arXiv:astro-ph/9802187v1 13 Feb 1998

Clues to Outflows: Polarization of IRAS-Selected QSOs

Beverley J. Wills

Astronomy Department, RLM 15.308, University of Texas at Austin, Austin TX 78712

Dean C. Hines

Steward Observatory, University of Arizona, 933 N. Cherry Ave. Tucson, AZ 85721

Abstract. Broad-band polarimetry and spectropolarimetry of a complete sample of 18 luminous AGNs ($L_{bol} \geq 10^{11.5} L_{\odot}$), selected in an orientation-independent way by warm infrared flux, shows that an orientation – dust-covering Unified Scheme like that successfully explored for the lower luminosity Seyfert galaxies applies to the luminous QSOs. Broad emission lines and continuum seen in polarized (scattered) light show that hyperluminous infrared galaxies contain buried QSO nuclei and are therefore the 'missing' QSO 2s – the high-luminosity analogs of Seyfert 2 galaxies like NGC 1068. Most of the QSOs show significant polarization and reddening. Three are 'classical' low-ionization BAL QSOs, and several others have narrower, blueshifted, low-ionization absorption. These properties are to be compared with those of the UV-optically selected QSOs, of which only ∼1% show low-ionization BALs, and only the BAL QSOs show significant polarization. Outflows are therefore much more common than previously suspected.

1. The Relevance of Polarized IRAS AGNs to Mass Ejection from AGNs

The fraction of luminous AGNs showing blueshifted absorption lines gives us the covering factor of the outflowing gas — but only if the sample is unbiased with respect to orientation. Polarimetry and spectropolarimetry allow us to detect buried QSOs in scattered light and thus to test orientation-dependent Unified Schemes for luminous AGNs, analogous to those for Seyfert nuclei.

The statistical relation of blue-shifted absorption lines to orientation-dependent obscuration and scattering, and a comparison of line and continuum absorption in transmitted and scattered light paths in individual objects, constrain the geometry and physical conditions in the absorbing gas.

We must first define an orientation-independent sample, and show that the QSO central engines are actually the same kind, despite the different appearances at different orientations.

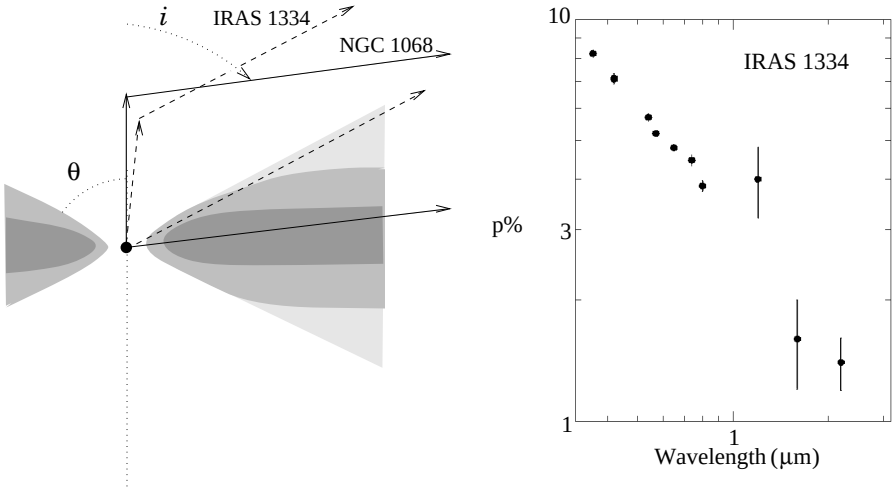

Figure 1. (a, left) Cross-section through a dusty torus surrounding a continuum source and broad line region (black dot). θ is the opening half-angle of the ionization or scattering cone formed by the shadow of the torus, and i is the inclination of the line-of-sight to the axis (shown for NGC 1068). Paths of scattered (polarized) and transmitted (reddened) light are shown for the buried Sy 1 in NGC 1068 (solid lines), and the less-obscured QSO IRAS 13349+2438 (dashed lines). (b, right): Wavelength-dependent polarization of IRAS 13349+2438.

1.1. How to Select an Orientation-Independent Sample

Unified Schemes successfully explain the diverse appearance of AGNs by means of different viewing angles of an axisymmetric system. Figure 1 illustrates the geometry deduced for the lower-luminosity AGNs (Seyfert nuclei), and some luminous IRAS AGNs (Antonucci & Miller 1985; Goodrich & Miller 1994, Wills et al. 1992; Hines & Wills 1993). The total light spectrum of NGC 1068 is dominated by starlight and a Seyfert 2 spectrum – strong, unpolarized narrow lines viewed directly, arising within the ionization cone. Viewed at inclination i, equatorial extinctions of perhaps several 100 in A_V effectively block the optical view of the central AGN ($\sim 10^m$ at 20 μm), but nuclear light scattered by electrons within the opening angle of the torus reveals a Seyfert 1 continuum and broad emission lines in polarized light. In contrast, the first IRAS-discovered high-luminosity AGN (QSO) IRAS 13349+2438 is viewed at a smaller i. The total light spectrum looks like that of a normal QSO, reddened, and with very weak narrow-line emission. However the percentage polarization p% is high and rises dramatically to the UV (Fig. 1b). This is a result of a normal unreddened QSO spectrum seen in scattered, polarized light, diluted by an unpolarized reddened spectrum of the QSO viewed directly, through absorbing dust.

UV-optical surveys are incomplete because they miss QSOs that lie within a dusty torus or are buried in a dusty galaxy. Despite high absorption along the line-of-sight, buried QSOs can be revealed in scattered (polarized) light.

Thus polarimetry and spectropolarimetry allow us to test Unified Schemes for luminous AGNs (QSOs) – to show whether the dusty hyperluminous infrared galaxies (HIGs) contain the same kind of active nucleus as the UV-optically selected QSOs.

The optically thick torus may intercept an appreciable fraction of the QSO's UV-optical luminosity. At a few pc from the QSO nucleus, dust grains will be heated to an equilibrium temperature of 1000 K, radiating near 3μm, and at $\sim$1 kpc, grains at 100 K will radiate near 30 μm. The dusty gas may generally be optically thin at mid-IR wavelengths. This allows an approximately orientation-independent sample to be selected by warm IR colors.

2. The Sample and Observations

The sample is shown in Table 1. The 12 QSOs were derived from the complete sample defined by Low et al. (1988) who selected sources from the IRAS Point Source Catalog with $|b| > 30°$, detected at 60 μm, and with $F_\nu(25\mu m)/F_\nu(60\mu m)$ >1/4. They present only the broad-emission line objects. We have selected those with $L(IR) > 10^{11.5} L_\odot$ (H_0 = 100 km s^{-1} Mpc^{-1}). We excluded radio core-dominant objects because their spectra are contaminated by synchrotron emission. We included two additional QSOs at the flux limit of Low et al.'s sample. From the literature, we added all 6 objects known to satisfy the same luminosity, flux, and IR color criteria as the Low et al. QSOs. All 6 show strong narrow-line emission. This is likely to be a lower limit to the true number of these HIGs.

We measured linear polarization in unfiltered light for the whole sample, using the Breger broad-band polarimeter on the McDonald 2.1-m Struve telescope. Objects showing significant p% were measured through filters – $CuSO_4$, RG630, and standard UBVRI bands. Spectropolarimetry for 3 QSOs and 3 HIGs was obtained using the LCS spectropolarimeter on the McDonald 2.7-m Smith telescope. Table 1 summarizes our results. Further details of our measurements, and data from other sources, may be found in Wills & Hines (in preparation), Hines (1994), and the references to Table 1.

3. Results

The sample AGNs are grouped in Table 1 in order of decreasing obscuration. On the axisymmetric dusty torus model of Fig. 1 this could be interpreted as decreasing inclination. The spectra of the first two groups (HIGs) are dominated by starlight and strong, Seyfert 2-like narrow lines. When corrected for starlight p% is high (up to 26%). The polarized flux spectra show reddened QSO continuum and BLR. In the first group the scattered light is even redder than starlight, resulting in a characteristic increase in p% to longer wavelengths. In contrast, in the second group, the scattered QSO continuum and broad lines are much less reddened, resulting in higher observed p% increasing towards the UV. All the remaining groups show QSO broad lines and continuum in total and direct light. In the third group the total spectrum is reddened but p% increases to the UV – a result of a reddened direct view of the nucleus but much less reddened scattered spectrum. p% is generally quite high. Narrow asso-

Table 1. Summary of Polarimetry Results[a]

Name	log L_{bol}[b]	Class	p_{max}%[c]	p_λ[d]	Absorbing Outflow[e]	Polarized Compnt[f]	New Class
IRAS 05189−2524	11.9	HIG	5.0±0.1	+	···	BLR,cont	QSO 2
IRAS 20460+1925	12.9	HIG	5.0 0.5	+	···	BLR,cont	QSO 2
IRAS 23060+0505	12.5	HIG	8.1 0.3	+	···	BLR,cont	QSO 2
IRAS 09104+4109	12.6	HIG	21.0 3.2	−	···	BLR,cont	QSO 2
IRAS F10214+4724	14.4	HIG	18 ...	−	···	BLR,cont	QSO 2
Mkn 463 E	11.8	HIG	13 ...	−	···	BLR,cont	QSO 2
I Zw 1	12.0	QSO	1.7 0.2	−	LOAL?	?,cont	QSO 1
Mkn 231	12.4	QSO	10.5 0.3	−	LOBAL,LOAL	BLR,cont	QSO 1
IRAS 13349+2438	11.6	QSO	8.0 0.2	−	LOAL?	BLR,cont	QSO 1
IRAS 14026+4341 (CSO 409)	12.1	QSO	12.0 0.7	−	LOBAL,LOAL	BLR,cont	QSO 1
IRAS 00275−2859	12.7	QSO	1.5 0.1	**0**	···	···	QSO 1
IRAS 07598+6508	11.8	QSO	2.2 0.1	**0**	LOBAL,LOAL	cont	QSO 1
PG 1700+518	11.9	QSO	0.5 0.1	−	LOBAL,LOAL	?,cont	QSO 1
IRAS 21219−1757	11.8	QSO	1.5 0.2	−	···	?,cont	QSO 1
PHL 1092	11.9	QSO	0.3 0.3	···	···	···	QSO 1
Mkn 1014	12.5	QSO	0.7 0.2	···	···	···	QSO 1
IRAS 04505−2958	12.0	QSO	0.4 0.2	···	···	···	QSO 1
IRAS 13218+0552	11.7	QSO	0.7 0.4	···	···	···	QSO 1

[a] The groups of objects are arranged in order of decreasing obscuration, or, on a model as in Fig. 1, decreasing inclination of the line-of-sight to the axis of symmetry, assuming that such an axis of symmetry can be defined for these QSOs, as it is in many Seyfert galaxies.

[b] The bolometric luminosity is in units of $L_\odot$, assuming $H_0 = 100$ km s^{-1} Mpc^{-1}.

[c] This gives the maximum observed polarization from broad-band data or spectropolarimetry.

[d] The wavelength dependence of polarization. The '+', '−', and '**0**' symbols refer to polarization increasing with wavelength, decreasing, or with little wavelength dependence, respectively. In some cases the observed p% is too small for the wavelength dependence to be defined.

[e] 'Absorbing Outflow' refers to the existence of blueshifted low-ionization absorption lines – either broad (LOBAL), or narrow (LOAL, Boroson & Meyers 1992 ApJ, 397, 442).

[f] 'Polarized Component' indicates which is seen in polarized flux – either the BLR or continuum.

References to polarization data are:

Berriman, G. , Schmidt, G. D. & West, S. C. 1990, ApJS, 74, 869 (Mkn 1014)

Hines, D., Schmidt, G., Smith, P., & Weymann, R. 1995, BAAS, 187, 8409 (PG1700+518)

Hines, D. C. & Wills, B. J. 1993, ApJ, 415, 82 (IRAS 09104+4109)

Hines, D. C. & Wills, B. J. 1995, ApJ, 448, 69L (IRAS 07598+6508)

Jannuzi, B. T., Elston, R., Schmidt, G. D., Smith, P. S., & Stockman, H. S. 1994, ApJ, 429, 49 (IRAS F10214+4724)

Kay, L. E. 1994, ApJ, 430, 196 (Mkn 463E)

Miller, J. S. & Goodrich, R. W. 1990, ApJ, 355, 456 (Mkn 463E)

Tremonti, C. A., Uomoto, A., Antonucci, R. R. J., Tsvetanov, Z. I., Ford, H. C., & Kriss, G. A. 1996, BAAS, 189, 1105 (Mkn 463E)

Smith, P. S., Schmidt, G. D., Allen, R. G., & Angel, J. R. P. 1995, ApJ, 444, 146 (Mkn 231)

Stockman H.S., Moore R.L., & Angel J.R.P. 1984, ApJ, 279, 485 (PHL 1092)

Webb, W., Malkan, M., Schmidt, G., & Impey, C. 1993, ApJ, 419, 494 (I Zw 1)

Young, S., Hough, J. H., Efstathiou, A., Wills, B. J., Bailey, J. A., Ward, M. J., & Axon, D. J. 1996, MNRAS, 281, 1206 (Mkn 463E, Mkn 231)

Wills, B. J., Wills, D., Evans, N. J., Natta, A., Thompson, K. L., Breger, M., & Sitko, M. L. 1992, ApJ, 400, 96 (IRAS 13349+2438)

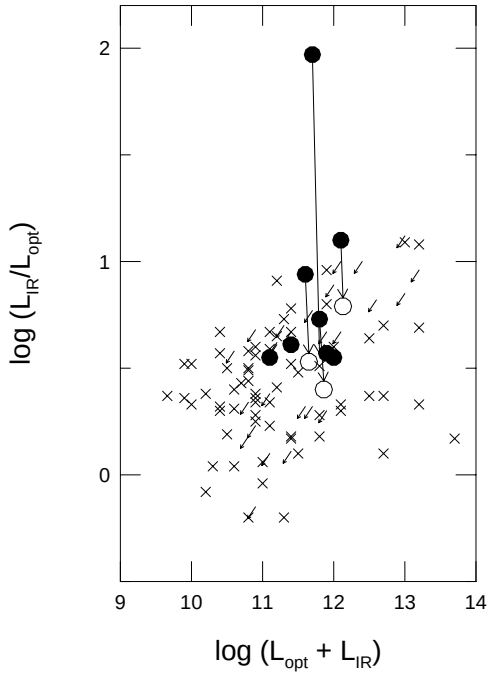

Figure 2. A comparison of log L_{IR}/L_{opt} for IRAS-selected QSOs (•), with optically selected PG QSOs (×, and upper limits) of the same bolometric luminosity. Reddening corrected values (○), show that IR-selected QSOs do not have enhanced L_{IR} compared with optically-selected QSOs. Figure adapted from Low et al. (1989).

ciated absorption or weak, broad absorption is seen in all these objects. The objects of the fourth group all have significant but low p% and at least 3 show low-ionization narrow and broad associated absorption. These spectra are less reddened than the preceding groups. At least in IRAS 07598+6508 the broad emission lines are unpolarized. Taking into account spectropolarimetry of other BAL QSOs as well, apparently a lower inclination view of the nucleus results in multiple (direct and scattered) views of the QSO nucleus. Finally, the QSOs of the fifth group appear as unpolarized, like nearly all of the 114 UV-optically selected PG QSOs (Berriman et al. 1990). On an axisymmetric torus model, these are relatively unobscured QSOs, viewed within the opening angle ($i < \theta$).

4. Interpretation

Broad-band polarimetry and spectropolarimetry of 12 QSOs and 6 HIGs selected by warm 60μm and 25μm flux densities, and therefore essentially unbiased with respect to orientation, shows that these are analogous to the Seyfert 1 and 2 classes at lower luminosities. Spectropolarimetry reveals QSO-like polarized broad emission lines and continua in all 6 HIGs. This means that a dust-orientation Unified Scheme holds for luminous AGNs, and the HIGs – the 'missing' QSO 2s – constitute ∼30% of this population.

The axisymmetric torus model is suggested by analogy with Seyfert nuclei where radio-jets, ionization cones or dust disks define the axis, and, for IRAS 13349+2438, by the major axis of its host galaxy. However, the sequence we have described could be simply one of decreasing dust content. If dust content were greater for the more reddened objects, we would expect their L_{IR} to be enhanced. A preliminary test of this is shown in Fig. 2 where we compare the ratio L_{IR}/L_{opt} for the Low et al. QSOs with that for the optically selected PG QSOs of the same bolometric luminosity. When corrected for line-of-sight reddening, L_{IR}/L_{opt} ratios are the same for the IR- and optically selected QSOs.

While the numbers are small and the number of HIGs is uncertain, from the different views at different inclinations we build a picture of a typical QSO as follows: $\sim$30% (6 HIGs) of the center is covered by thick dust, $\sim$40 – 45% by thinner dust (groups 3 & 4), with 20 – 25% of the QSO relatively unobscured (the 5th group). Blueshifted absorption lines are associated with partially obscured views of the nucleus. Only 3-4 QSOs are sufficiently unobscured to have been selected in UV-optical QSO surveys, so the true space density of QSOs has been underestimated by a factor $\sim$5. Webster et al. (1995) estimate that a similar fraction of radio-loud quasars (80%) have been missed as a result of reddening.

On the axisymmetric torus model we can assign a relatively clear view within a cone of $\theta \sim 22°$, a partially obscured zone with low-ionization absorbing outflows between $\theta \sim 22°$ and 50°, and a thick dusty torus with $\theta \sim 50°$. These numbers are consistent with half-opening angles deduced from spectropolarimetry of individual objects of the sample (see references in Table 1).

Low-ionization absorbing outflows are related to dusty gas – neutral and warm (see Grupe et al., Mathur, this volume) – and, whichever dust-orientation Unified Scheme holds, they are much more common than previously thought[1].

Acknowledgments. We thank D. Wills, M. Breger, J. H. Hough, R. W. Goodrich, D. R. Doss, E. Dutchover and V. Vats (Karl Lambrecht Corporation) for observing and instrumentation help, and NASA (grant NAG5-3431).

References

Antonucci, R. R. J., & Miller, J. S. 1985, ApJ, 297, 621

Berriman, G. , Schmidt, G. D. & West, S. C. 1990, ApJS, 74, 869

Goodrich, R. W., & Miller, J. S. 1994, ApJ, 434, 82

Hines, D. C. 1994, PhD thesis, University of Texas

Hines, D. C. & Wills, B. J. 1993, ApJ, 415, 82

Low, F. J., Huchra, J. P., Kleinmann, S. C., & Cutri, R. M. 1988, ApJL, 327, L41

Low, F. J., Cutri, R. M., Kleinmann, S. C., & Huchra, J. P. 1989, ApJL, 340, L1

Webster, R. L., Francis, P. J., Peterson, B. A., Drinkwater, M. J., & Masci, F. J. 1995, Nature, 375, 469

[1]In related work, Hines & Schmidt (these Proceedings) use polarization of a large sample of BAL QSOs to investigate their relation to HIGs.

Wills, B. J., Wills, D., Evans, N. J., Natta, A., Thompson, K. L., Breger, M., & Sitko, M. L. 1992, ApJ, 400, 96

Discussion

Kirk Korista: Are all the BAL QSOs in your sample Mg II-type BAL QSOs? Would you know whether your sample included high-ionization ("normal") BAL QSOs?

Bev Wills: The sample QSOs, being IRAS-selected, are all low redshift, so any information on the (UV) high-ionization BALs must come from IUE or HST spectroscopy. In all cases for which that information is available, objects with low-ionization BALs also show high-ionization BALs. I do not know any exceptions to this. Apart from the objects in our sample that we know have low-ionization absorption, I don't think that UV spectroscopy is available. UV spectroscopy would provide an important clue to the relation between low-ionization and high-ionization-only broad absorption line gas, with or without axisymmetric torus models (see Weymann, Morris, Foltz, & Hewett 1991, ApJ, 373, 23).